

# **Extending The Barrowman Method For Large Angles Of Attack**

Research and Development Project  
submitted at NARCON March 1999,

By

Edward V. LaBudde

NAR # 73451

1768 Upper Ranch Road  
Westlake Village, CA 91362  
805-495-6726 Phone/Fax  
E-mail: evl@pobox.com

## Abstract

### Extending The Barrowman Method For Large Angles Of Attack

By Edward V. LaBudde NAR # 73451

The original Barrowman method for predicting the center of pressure is valid only at zero angle of attack because it neglects the effects of the body on aerodynamic properties. We desire to extend the Barrowman method for large angles of attack, consequently, we have created a set of hypotheses for do so. These assumptions use the data developed by both the original Barrowman method as well as the “standard cutout” method in estimating the aerodynamic properties. The hypotheses ensures that the values for center of pressure and normal forces match the Barrowman method at zero degrees and the cutout method at 90 degrees. The hypotheses assume that changes in the center of pressure and normal forces can be estimated by the use of a sine law of projected area of the body. Additionally, we extended the basic Barrowman calculations by including the body interference factor neglected by Barrowman in the original work.

These assumptions are contrary to the conventional non-linear lift theory. This theory is called non-linear because the lift is a function of  $\sin^2(\alpha)$ . Non-linear lift originates on the body due to viscous effects. The new model, however, matches the wind tunnel data better

The new model allows a good estimate of the pitching moment up to 45 degrees, thus making it useful for exploring dynamic stability problems using time domain simulations and analysis. The point of positive pitching moment (instability) can be estimated by the new model, and making it useful as a top-down budgeting tool.

Future work will use this model in a top-down design procedure that will maximize altitude performance in the presence of wind, thrust and airframe errors.

## Table of Contents

<b>Abstract</b> .....	2
<b>Table of Contents</b> .....	3
<b>List of Figures</b> .....	3
<b>Introduction</b> .....	4
<b>Symbols</b> .....	4
<b>Background</b> .....	4
Non-linear Aerodynamic Theory .....	5
<b>Analysis</b> .....	5
Extending the Barrowman Method .....	6
Hypothesis #1 .....	6
Hypothesis #2 .....	6
Hypothesis #3 .....	6
Hypothesis #4 .....	7
<b>Results -Wind Tunnel Validation</b> .....	8
<b>Discussion of Results</b> .....	11
Stall Angle of Attack .....	12
Properties of Finless Rockets .....	12
Properties of Unstable Finned Rockets .....	13
Properties of Stable Finned Rockets .....	13
<b>Conclusions</b> .....	13
<b>Equipment and Cost</b> .....	14
<b>Acknowledgments</b> .....	14
<b>References</b> .....	14
<b>Appendix I</b> .....	15

## List of Figures

Figure 1 General Shape of Pitching Moment .....	8
Figure 2 Long Arcas Body Pitching Moment .....	9
Figure 3 Long Arcas Finned Data .....	10
Figure 4 Long Arcas Center of Pressure .....	10
Figure 5 Budget Model .....	11

## Introduction

The objective of this R&D report is to create a model that extends the classical Barrowman method of the center of pressure prediction for large angles of attack. We strive to generate a valid expression for the aerodynamic properties for  $\alpha$  up to a range of at least 20-30 degrees. The approach also unifies the Barrowman and standard cutout methods of  $C_p$  prediction. The value of this model will be to help define limits for angle of attack excursions for dynamic stability considerations.

## Symbols

$\alpha$  = Angle of attack

$A_f$  = Lateral area of fins

$C_d$  = Drag coefficient

$C_g$  = Center of gravity

$C_L$  = Lift Coefficient

$CLA_b$  = Center of pressure of the body alone by the cutout method

$C_m$  = Pitching moment

$C_{Na}$  = Barrowman normal force coefficient for complete rocket

$C_{Nab}$  = Barrowman normal force coefficient for body alone at zero  $\alpha$

$C_{Nac} = C_d * \text{lateral area} / \text{frontal area}$ , normal force coefficient for body alone by the cutout method

$C_p$  = Barrowman center of pressure of the complete rocket at any  $\alpha$

$C_{pb}$  = Barrowman center of pressure of the body alone at any  $\alpha$

$C_{po}$  = Barrowman center of pressure of the complete rocket at zero  $\alpha$

$C_{pob}$  = Barrowman center of pressure of the body alone at zero  $\alpha$

$L$  = Lift force

$Q$  = Dynamic pressure =  $\frac{1}{2} \rho V^2$

$\rho$  = Air density

$S_{ref}$  = Reference Area

$V$  = Free stream Velocity

## Background

Our motivation for this work was driven out of a desire to find a design procedure that would assure maximum altitude performance. We recognize that many of the usual design rules used by model builders produce designs that are over stable and fly at reduced altitudes. Further, we believe that, for a given set of specifications on parameters affecting flight stability (i.e. wind, thrust and airframe misalignment), there is an optimum fin design that will achieve the highest altitude.

Prior to the publication of the now famous “Barrowman” method [1] on the prediction of the center of pressure, model rocketeers had limited methods of  $C_p$  determination. One method called the “Standard Cutout Method” involved cutting out the planform of the rocket made of cardboard and locating the center of gravity, the assumed center of pressure. This method is valid for angles of attack ( $\alpha$ ) of 90 degrees. Until now, it has not been very useful for the normal  $\alpha$

encountered by the typical model rocket. This method has been largely displaced by the Barrowman method.

James S. and Judith A. Barrowman published their landmark paper in August 1966, and it has become the “Holy Grail” of model rocketry. The method is derived assuming potential flow theory, neglecting viscous flow and vortex formation, using the sub-sonic pressure coefficient. The method estimates the normal force coefficient,  $C_{Na}$ , as well as the location of the center of pressure,  $C_p$  (or  $X_r$ ), for the rocket. For most model rocket designs, it is valid only at ZERO  $\alpha$ . Substantial errors in forces and center of pressure can arise even for a few degrees of  $\alpha$ . Despite these limitations, it has endured as the method of choice for most model rocket enthusiasts.

The assumptions that went into the original Barrowman method excluded any contribution of body lift. This resulted from the assumption that the pressure coefficient is a function of the rate of change of cross sectional area. The body tube has none, and therefore is ignored by the calculations. This assumption is true only at ZERO  $\alpha$ .

### Non-linear Aerodynamic Theory

A real body produces lift due to viscous effects as the angle of attack increases (also known as non-linear lift because it varies as  $\sin^2(\alpha)$ ). A pair of vortices are formed over a streamlined body, just as in low aspect ratio wings, which reduces the pressure distribution on the aft body. Under this condition, the lift is generated mainly by the fore body.

Hoerner [2] discusses the non-linear cross flow forces in his chapter on lift of bodies (19) and the movement of the aerodynamic center with angle of attack. Generally, the non-linear normal force coefficient is defined as  $C_n = k \sin^2(\alpha)$ , where  $k$ , represents the drag coefficient, and can be anywhere from .2 to over 2. The reference area is the lateral area of the body (similar to the cutout method), being about .6-.8 of length\*diameter. Hoerner suggests that the lift force acts on the center of the cylindrical body.

We were unable to produce a useful fit to the wind tunnel data using the cross flow theory.

### Analysis

In any discussion of large  $\alpha$ , the first order of business is to remove any small angle assumptions built into the standard aerodynamic model. Traditionally aerodynamists use small angle approximations in estimating aerodynamic forces and moments. A typical model for the lift generated by an airfoil is given by:

$$L = Q S_{ref} C_L a \quad (1)$$

If the airfoil is pitched to an  $\alpha$  of 2 Pi radians it would be facing into the airflow at zero  $\alpha$  and would not produce any lift. The above model would lead us to believe that large amounts of lift are generated. To avoid this error, it is necessary to replace  $\alpha$  with  $\sin(\alpha)$  everywhere it appears in aerodynamic formulas.

## Extending the Barrowman Method

The original Barrowman assumptions lead to a *first order* approximation to the aerodynamic properties (i.e.,  $C_{Na}$  is the *slope* of the pitching moment at zero  $\alpha$ ). To arrive at a *second order* approximation it will be necessary to incorporate the body effects on the aerodynamic performance. We seek a gross approximation to the actual shape of the pitching moment. That is, the general shape up to the point of stall, the stall point and the point of zero pitching moment. These hypotheses are novel in that they transform the *outputs* of the Barrowman and cutout methods, rather than modify the internal calculations. The use of a sine law transformation insures that the Barrowman parameters will be achieved at zero angle of attack and the cutout parameters at 90 degrees.

### Hypothesis #1

We have postulated that the  $C_p$  of a finless rocket composed of a nose and cylindrical body can be approximated by using the sine law of projected area of body and knowing the center of pressure by the Barrowman AND cutout method:

$$C_{pb} = C_{pob} + \sin(|a|) (CLA_b - C_{pob}) \quad (2)$$

### Hypothesis #2

We have postulated that the normal force coefficient for the body will follow the sine law as well:

$$C_{N_{ab}} = C_{N_{aob}} + \sin(|a|) (C_{N_{acb}} - C_{N_{aob}}) \quad (3)$$

The pitching moment for a finless body then becomes:

$$C_m = C_{N_{ab}} (C_g - C_{pb}) \sin(a) \quad (4)$$

The resulting pitching moment of the body alone becomes cubic in  $\sin(\alpha)$ .

When fins are added to the rocket the  $C_p$  changes to the location estimated by the original Barrowman method (here referred to as  $C_{po}$ ). The change in location of the  $C_p$  with increasing  $\alpha$ , however, must be the same as for the body alone. This is because the location of the  $C_p$  of the nose and fins are not assumed to be a function of  $\alpha$ , although all airfoils have limits to the  $\alpha$  that can be tolerated before they stall. Therefore any variation in  $C_p$  with  $\alpha$  must be associated with the body. This leads to the third hypothesis.

### Hypothesis #3

We have postulated that the  $C_p$  of the finned rocket must shift by the same amount as the body alone, leading to the  $C_p$  of a finned rocket to become:

$$C_{pf} = C_{po} + \sin(\alpha) (CLA_b - C_{pob}) \quad (5)$$

The pitching moment of the finned rocket up to the stall angle then becomes:

$$C_m = C_{Na} (C_g - C_{pf}) \sin(\alpha) \quad (6)$$

As shown, the pitching moment will now be second order in  $\sin(\alpha)$ , becoming a *second order* approximation to pitching moment. We shall see later that this is a significant improvement in accuracy. Equation (6) is valid up to the value of  $\alpha$  at stall. When the fins stall it is assumed that they no longer have any significant influence in the pitching moment and therefore can be ignored.

It is well known that most simple airfoils will stall at an  $\alpha$  of about 10-20 degrees. The empirical data shown by Hoerner in his section on low aspect ratio wings (17) suggests that the stall angle is a function of the fin aspect ratio. An approximation to the data presented leads to an estimate of the stall angle in degrees as:

$$a_{Stall} = 15 \left( 1 + \frac{1.1}{AR} \right) \quad (7)$$

$$AR = \frac{(Span)^2}{A_F}$$

Note that the body of the rocket must be included in the total lateral area,  $A_F$ , of the fins, and the span between fin tips.

This leads us to the fourth hypothesis.

#### Hypothesis #4

We have postulated that the pitching moment will follow the body pitching moment after the fins stall. At the point of stall, the pitching moment reaches its maximum value. It then decreases in value and might even change sign, becoming unstable. After stall, the pitching moment will revert to equation (4), but it will be offset by an amount equal to the value of the difference between the finned rocket and the body alone. In effect, the body pitching moment has been displaced downward by this difference. The resulting shape of the pitching moment with  $\alpha$  will resemble that shown in Figure 1, if the rocket is stable at zero  $\alpha$ :

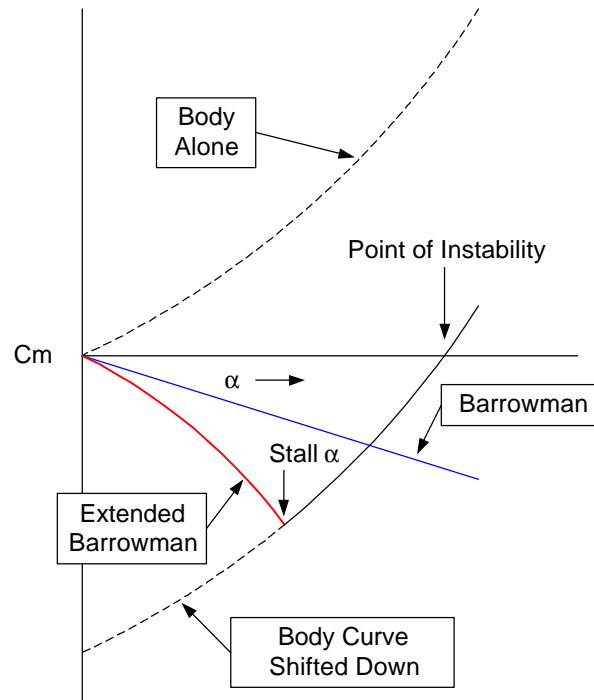


**Figure 1 General Shape of Pitching Moment**

These set of hypotheses produce a model that will be substantially more accurate at large angles of attack than the original Barrowman estimate. Of course, this model would never be capable of predicting the nuances seen in actual wind tunnel data. However, it can be used as a good approximation to the dynamic behavior for simulation and analysis purposes. Most significant, this model can be used to estimate the point of instability, which is a major consideration for fin design.

Before moving on, we would like to make an extension to the original method. The Barrowman's left out the interference factor for the body in the original work, concluding that it could be neglected for a typical model rocket (and to be conservative). This factor can be significant for a rocket with small fins. Figure 7 in [1] shows the curve for  $k_B(T)$ . Given the tail radius,  $rt$ , and semi span,  $s$ ,  $SR = rt/(s+rt)$ , a regression analysis approximates the curve as:

$k_B(T) = .7809 * SR^2 + 1.2SR$  This term is added to the fin-body interference factor  $k_T(B)$ .

### Results -Wind Tunnel Validation

The above hypotheses were compared to actual wind tunnel data to test the validity. A paper presented by Tom McAtee [4] at NARAM-40, provided some data needed to validate the model. A copy of the pitching moment for the Long Arcas is shown in Appendix 1. Our first order of business was confirming hypotheses #1 and #2, the pitching moment for the body alone. We normalized the rocket dimensions to 13.818mm diameter in case we wanted to flight test it with an Estes mini-engine. We constructed a spreadsheet, AERO.XLS, to generate numerical results from the model. The spreadsheet performs all the Barrowman and cutout method calculations as

well as the new models, totaling over 60 calculations in all. The model takes dimension data inputs and results in pitching moment and other useful parameters. The present model has the stall angle as an input rather than using equation (7).

The results for the Long Arcas body are shown in Figure 2 below. It was necessary to use the original Barrowman method rather than the “extended” method using the body interference term. It is not clear why the extended method failed in this example. The goodness of fit,  $R^2$ , is .999. An estimate of the drag coefficient for the body at a Reynolds number of  $7.8 \times 10^6$  is about .44, however, the drag coefficient for calculating  $C_{nac}$  was .425 for the best fit to data. In order to achieve this fit, a “fudge factor” of 1.15 was applied to the rear diameter of the boat tail. It is assumed that there might be a flow separation problem at the rear of the actual wind tunnel model. All other parameters were per Long Arcas data.

Note that the pitching moment shows a significant curvature upwards, due to the combined effects of the correction of both the normal force coefficient as well as the center of pressure variation with  $\alpha$ .

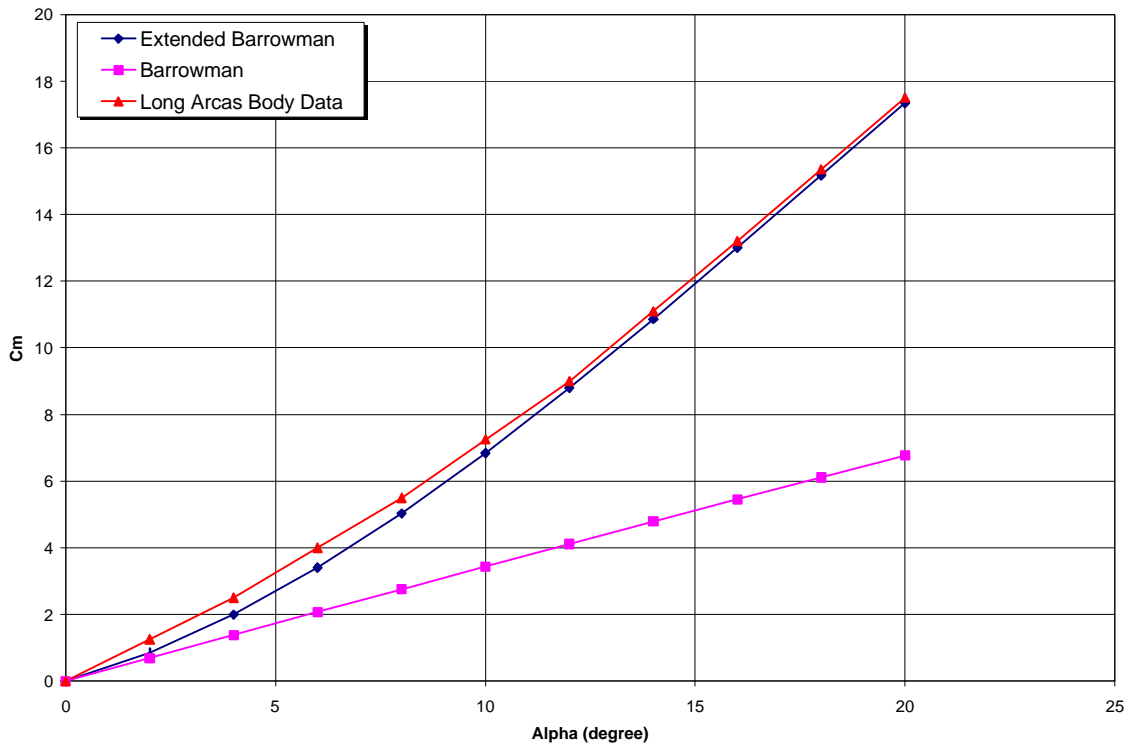


**Figure 2 Long Arcas Body Pitching Moment**

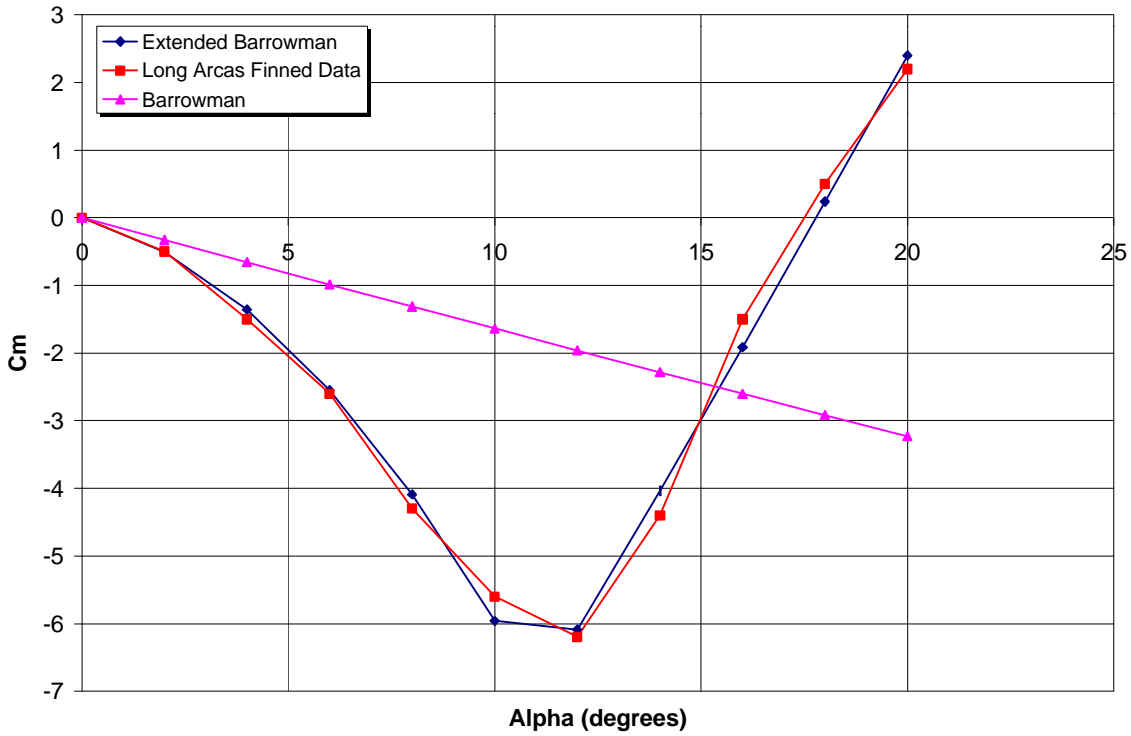


**Figure 3 Long Arcas Finned Data**

The fit to the finned rocket is shown in Figure 3 above. The data used is the Mach .6, zero incidence condition. The overall goodness of fit is  $R^2=.99$ . The same “fudge factor” was used in this data, and the assumed stall angle was 11 degrees. We were surprised that the stall angle was so low, given the Hoerner data would suggest a value over 20 degrees. Perhaps the  $2\alpha$  flow around the body causes the fins to stall sooner. As shown, there is a significant departure from a straight line in the extended Barrowman and the actual data. The pitching moment becomes

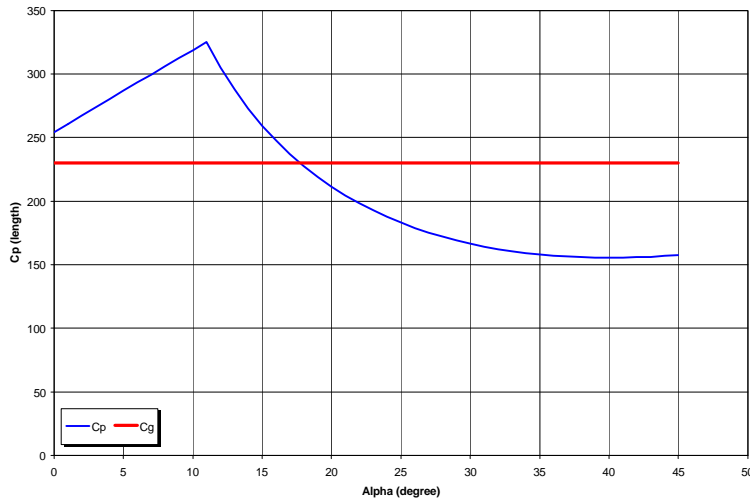


**Figure 4 Long Arcas Center of Pressure**

positive around 18 degrees. At that point, the moment will push in the wrong direction and become unstable. The movement of the location of center of pressure for the long Arcas is shown in Figure 4 above. Note that the  $C_p$  crosses the  $C_g$  at the point of positive pitching moment.

## Discussion of Results

The value of the extended Barrowman model cannot be overstated. It not only estimates the  $C_p$  location and force coefficient as a function of  $\alpha$ , it also estimates the point at which the pitching moment becomes unstable. The extended Barrowman model is exactly what is needed for dynamic stability analysis and simulations. The new model will provide better accuracy in predicting the dynamic response in time domain multiple degree of freedom simulations. More importantly it provides a budgeting tool for allocating the effects of wind, thrust and airframe misalignment. If the angle of attack due to each of these effects can be calculated, they must all fit with in the point of zero crossing, with some margin for safety, or the rocket will become unstable. (It should be noted that it is possible to operate the rocket up to the point of positive pitching moment without stability concerns. After the fins stall there will be a significant rise in drag, so a price in excess energy loss will be paid). This concept is shown in Figure 5 below. Flight simulations on typical model rockets suggest that keeping the maximum peak  $\alpha$  below the point of positive pitching moment will guarantee stability. The simulations show that a typical model rocket will reach the maximum  $\alpha$  shortly after clearing the launcher and will quickly move into the stable region within a few dozen milliseconds.

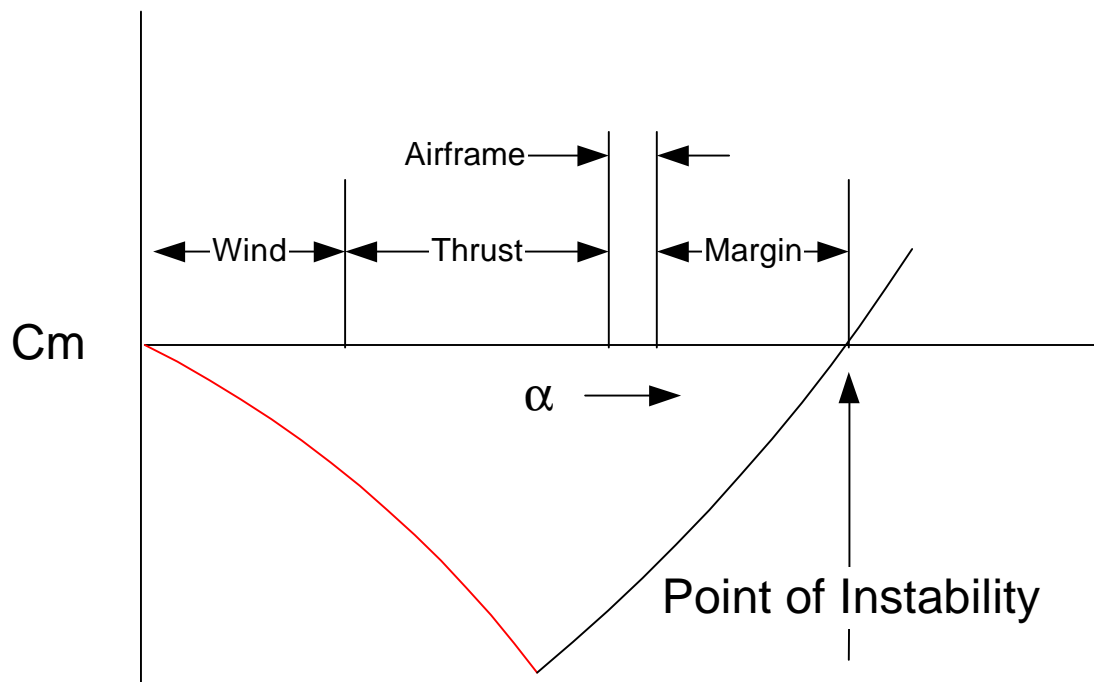


Figure 5 Budget Model

By using this budgeting concept, it is possible to define a top-down procedure by which one can guarantee that acceptable limits are met, with regards to ensuring that the disturbances are properly dealt with as well as maximizing altitude performance. That is precisely the focus of our yet-to-be published R&D paper [5].

Using the Long Arcas rocket as an example, the point of positive pitching moment is about 18 degrees. If we wish to prevent unstable operation, we would select a suitable margin of about 5 degrees. That will leave about 12 degrees to be allocated to wind, thrust and airframe errors. If we allow a modest amount for air frame errors of about 2 degrees, we are left with wind and thrust to total 10 degrees. If we assume that we allocate 5 degrees equally to wind and thrust, we have a complete budget. We could use this budget to design a fin set that would ensure we meet the requirement.

There is a trade off in fin design for effects of wind and thrust. The larger the fin, the less thrust errors, but, the larger the weathercock effects. Unfortunately, our model shows that by using small fins to avoid weathercock may be bad advice. Small fins will have low values  $\alpha$  at positive pitching moment. Thus a rocket with small fins may not weathercock as much, but it could go UNSTABLE in the wind, making it dangerous to fly!

### Stall Angle of Attack

The value for the stall angle of attack in the analysis of the Long Arcas was 11 degrees to match the data. Generally one could expect the actual value to be found anywhere from 10 to 20 degrees or more. To be conservative at estimating the positive cross over point, a value of 10-11 degrees should be used, as it might be a worst case limit.

### Properties of Finless Rockets

The foregoing analysis suggests that all finless rockets will be unstable at low angles of attack. If the center of pressure by the cut out method lies behind the center of gravity, it is possible to achieve stability at some large angle of attack. From equation (1), the point of stability will be reached when the center of pressure reaches the center of gravity as:

$$a_{Stable} = \sin^{-1} \left( \frac{C_g - C_{Pob}}{CLA_b - C_{Pob}} \right) \quad (8)$$

Any source of disturbance will drive the angle of attack to the stable point, causing a substantial turning maneuver. With typical model rocket designs, it is difficult to achieve a stability angle of much less than about 20 degrees, resulting in very erratic, and dangerous flight paths.

This behavior was confirmed by our own testing of finless rockets, including “stomp rockets.” We tested finless stomp rockets that had a  $C_g=94\text{mm}$ ,  $C_{pob}=7.2\text{ mm}$ , and  $CLA_b=122\text{ mm}$ . Using equation (8) we find that the point of stability is reached when the angle of attack is about 49 degrees. Actual stomp rockets were seen to be flying at angles of attack of about 30-40 degrees (eyeball measurements) and making large arcing flights in random directions.

## Properties of Unstable Finned Rockets

Finned rockets that are unstable at zero  $\alpha$  can become stable at some angle of attack, similar to finless rockets. Since the center of pressure will move aft with increasing  $\alpha$ , it will move to the point of stability. Modifying equation (8) for this condition, the point of stability will be reached when the center of pressure reaches the center of gravity as:

$$a_{Stable} = \sin^{-1} \left( \frac{C_g - C_{Po}}{CLA_b - C_{Pob}} \right) \quad (9)$$

In the case of the Long Arcas, the point of unstable operation is reached when the fin span is less than 10.25. It is possible to adjust the design to achieve any point of stability between zero and the stall angle, although it would be a dangerous rocket to fly!

## Properties of Stable Finned Rockets

Finned rockets that are stable at zero angle of attack do not necessarily reach a point where the pitching moment becomes positive. It is possible to place sufficiently large fins on the rocket so that it is stable beyond 45 degrees angle of attack. In the case of the Long Arcas, a fin span 27 will not produce an unstable cross over up to 45 degrees.

## Conclusions

We have constructed a set of hypotheses which will extend the Barrowman method to angles of attack up to at least  $\pm \pi/4$  radians. We have validated these assumptions with wind tunnel data with reasonably good results. The new model allows for the prediction of the point of positive pitching moment, making it an important budgeting tool for a top-down design procedure. Of some interest to old time rocket makers, the new model ties together the “standard cutout method” with the more modern Barrowman method, making a unified approach to modeling large angle of attack conditions.

Despite an excellent fit to wind tunnel data ( $R^2 > .99$ ), there were a few unexpected results. First, the extended calculations using the body interference factor did not yield acceptable results for the Long Arcas wind tunnel data. We do not have an explanation for this result. Second, a small “fudge factor” of 15% was needed to increase the aft diameter of the boat tail for the best match. We believe that flow separation problems on the wind tunnel model could explain this result. Third, the stall angle of attack of the wind tunnel data was only 11 degrees, whereas the low aspect ratio fins should have been around 20 degrees. One possible explanation for this could be the  $2\alpha$  flow around the body that would expose the fins to a higher angle of attack and make it stall sooner.

Individuals having more interest in exploring the Extended Barrowman method are encouraged to download the companion spreadsheet from the Apogee Components web site (<http://www.ApogeeRockets.com>).



**Appendix I**  
**Long Arcas Wind Tunnel Data from McAtee [4] (with permission).**

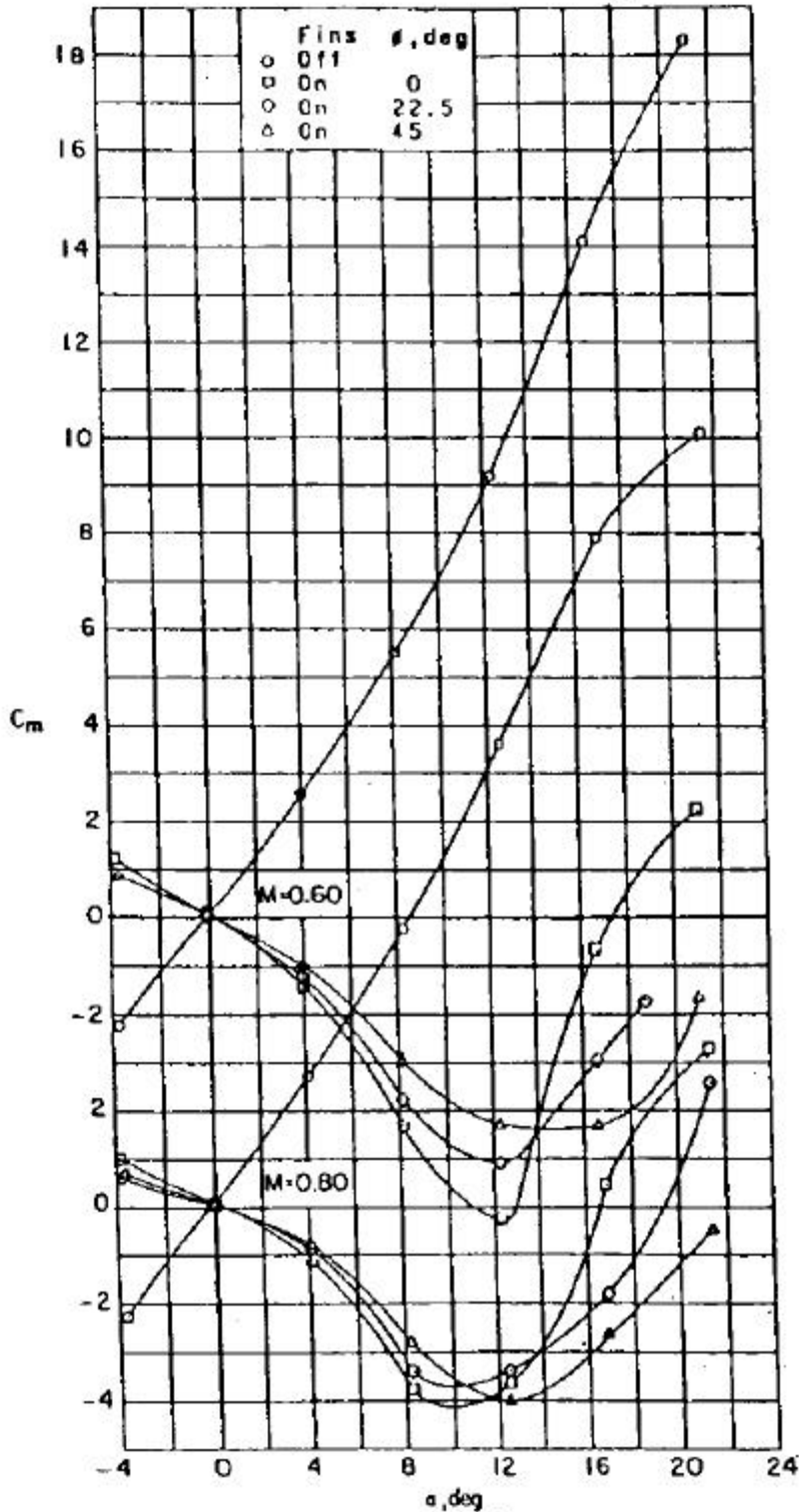


**FIGURE 4**

Pitching-moment coefficient.